ELSEVIER

Surface Science 490 (2001) 20–28

SURFACE SCIENCE

www.elsevier.com/locate/susc

Surface core-level shifts at an oxygen-rich Ru surface: O/Ru(0 0 0 1) vs. RuO_2(1 1 0)

Karsten Reuter *, Matthias Scheffler

Fritz-Haber-Institut der Max-Planck-Gesellschaft, Faradayweg 4-6, D-14195 Berlin-Dahlem, Germany

Received 14 April 2001; accepted for publication 25 May 2001

Abstract

We present density-functional theory calculations of Ru 3d and O 1s surface core-level shifts (SCLSs) at an oxygen-rich Ru(0 0 0 1) surface, namely for the O(1 × 1)/Ru(0 0 0 1) chemisorption phase and for two surface terminations of fully oxidized RuO_2(1 1 0). Including final-state effects, the computed SCLSs can be employed for the analysis of experimental X-ray photoelectron spectroscopy (XPS) data enabling a detailed study of the oxidation behaviour of the Ru(0 0 0 1) surface. We show that certain peaks can be used as a fingerprint for the existence of the various phases and propose that the long disputed satellite peak in RuO_2(1 1 0) XPS data originates from a hitherto unaccounted surface termination.

Keywords: Density functional calculations; X-ray photoelectron spectroscopy; Oxidation; Surface structure, morphology, roughness, and topography; Ruthenium; Oxygen; Single crystal surfaces

1. Introduction

In addition to the long-standing interest in RuO_2 as a technologically relevant metallic oxide per se, this material has recently also received a lot of attention as the end product in the oxidation sequence of ruthenium surfaces [1–4]. Epitaxially well oriented, incommensurate RuO_2(1 1 0) domains were identified on Ru(0 0 0 1) after heavy oxygen exposure and related to the enhanced catalytic activity towards CO oxidation [3,5], observed at Ru under high oxygen partial pressure [1,6]. Subsequently, an atomistic mechanism for this surface-oxide formation was proposed [7], in which after the completion of the full monolayer O(1 × 1) chemisorption phase on the surface, O penetrates into the sample and clusters in islands between the first and second metallic layer, locally decoupling a O–Ru–O trilayer from the underlying substrate. The ongoing oxidation results in more and more of these trilayers, which finally unfold into the more open rutile structure giving rise to (1 1 0) oriented RuO_2 patches on the surface.

Depending on the O partial pressure, a real Ru(0 0 0 1) surface will therefore exhibit a rather complex morphology, ranging from chemisorbed O overlayers to sub-surface O and RuO_2(1 1 0) patches with different surface terminations. Given this low degree of structural order, X-ray photoelectron spectroscopy (XPS) appears as a well suited tool to study the oxidation process in detail. However, the complex core-level spectra to be

* Corresponding author. Tel.:-49-30-8413-4821; fax: +49-30-8413-4701.

E-mail address: reuter@fhi-berlin.mpg.de (K. Reuter).

0039-6028/01/$ - see front matter
PII: S0039-6028(01)01214-6

expected from such a surface with a manifold of peaks due to coexisting domains will render the interpretation of the obtained data not unambiguous. This is even aggravated by the fact, that already for the $RuO_2(1\,1\,0)$ surface alone the origin of the peaks has been discussed controversially [8–15].

To provide a theoretical guidance for the experimental data analysis, we thus calculated all Ru 3d and O 1s surface core-level shifts (SCLSs) for the individual, already identified domains on an oxygen-rich Ru(0 0 0 1) surface, namely the $O(1 \times 1)$ chemisorbed phase, as well as two different surface terminations of $RuO_2(1\,1\,0)$. With this, we will show that certain peaks may be used as a fingerprint for the existence of one or the other domain.

2. Theoretical

The SCLSs are obtained from density-functional theory (DFT) calculations within the generalized gradient approximation (GGA) of the exchange-correlation functional [16]. The full-potential linear augmented plane wave method (FP-LAPW) [17–19] is used to solve the Kohn–Sham equations. We model the $O(1 \times 1)$/Ru(0 0 0 1) surface with a six layer slab, adsorbing O on both sides to preserve mirror symmetry. Likewise, the $RuO_2(1\,1\,0)$ surface is represented by a symmetric slab consisting of three rutile O–(RuO)–O trilayers. A vacuum region of ≈11 Å was employed to decouple the surfaces of consecutive slabs in the supercell approach. The resulting, fully relaxed geometries are in very good agreement with previous LEED and DFT studies [3,20].

The FP-LAPW basis set is taken as follows: $R_{MT}^{Ru} = 1.8$ bohr, $R_{MT}^{O} = 1.3$ bohr, wave function expansion inside the muffin tins up to $l_{max}^{wf} = 12$, potential expansion up to $l_{max}^{pot} = 4$. The Brillouin zone integration for the $O(1 \times 1)$/Ru(0 0 0 1) and $RuO_2(1\,1\,0)$ was performed using a $(12 \times 12 \times 1)$ and $(5 \times 10 \times 1)$ Monkhorst–Pack grid with 19 and 15 **k**-points in the irreducible part respectively. The energy cutoff for the plane wave representation in the interstitial region between the muffin tin spheres was 17 Ry for the wave functions and 169 Ry for the potential.

The SCLS, Δ_{SCLS}, is defined as the difference in energy which is needed to remove a core electron either from a surface or from a bulk atom [21,22]. We calculate this quantity both in the initial-state approximation, as well as taking final-state effects into account. In the prior approximation, the SCLS is simply due to the variation of the orbital eigenenergies before the excitation of the core electron. Yet, the total, measurable SCLS involves an additional component due to the screening contribution from the valence electrons in response to the created core hole. We obtain this total shift, Δ_{SCLS}^{total}, via the Slater–Janak transition state approach of evaluating total energy differences [23,24] using impurity type calculations where an ionized atom is once placed at the surface and once in the bulk. In order to decouple these ionized atoms from each other, we surround them with neighbours possessing the normal core configuration by performing the calculation in a (2×2) and a (2×1) supercell for Ru(0 0 0 1) and $RuO_2(1\,1\,0)$ respectively. Having calculated both the total and the initial-state SCLS allows us then to single out the final-state effect from their respective difference. The procedure and numerical accuracy of both types of calculations has been described in detail in a recent publication addressing the SCLSs of all ordered O adlayers on Ru(0 0 0 1) [25]. Comparing with a large set of experimental high-resolution core-level shift data we achieved consistent agreement to within $\approx\pm$ 0.05 eV, confirming the high accuracy and predictive nature of our calculations.

However, we immediately stress that we do not expect such a precision when comparing metallic with oxidic core levels. SCLSs are obtained from the difference between a surface and a bulk calculation and thus benefit from error cancellation, if both calculations are done on the same substrate (which eletronic structure may be equally well described by DFT–GGA) and within the same supercell. While this is obviously not the case for Ru vs. RuO_2, notice that the focus of the present work is also not the explanation of a highly accurate existing data set on a very well defined sample. Rather, we intend to provide a fingerprint

guidance for the XPS trends on an oxidizing Ru surface, where none of the conclusions drawn will be affected by a likely $\approx\pm 0.2$ eV inaccuracy between the position of the Ru and RuO_2 bulk peaks.

3. $O(1 \times 1)$/Ru(0 0 0 1) and RuO_2(1 1 0) surface structure

The initial oxygen chemisorption on the Ru(0 0 0 1) surface proceeds via four ordered adlayer structures, in which with increasing coverage O consecutively occupies the four available hcp sites of a (2×2) unit cell [26,27]. Sub-surface O penetration does not begin until the full $O(1 \times 1)$ monolayer has been completed [7,20,28], which is why only the latter adphase may coexist with already fully oxidized patches under O-rich conditions [4]. In the $O(1 \times 1)$, every Ru surface atom, $Ru^{chem,3f}$, is coordinated to three chemisorbed oxygens, O^{chem}, with a bond length of 1.97 Å (cf. Fig. 1a). Note, that we will use a nomenclature for the surface Ru atoms, where apart from a site specific characterization (e.g. chem for the chemisorption phase) also the number of direct O neighbours (e.g. 3f for threefold coordination) is indicated. Viceversa, we indicate for the surface O atoms to which specific site they bind (e.g. O^{chem} binds to the $Ru^{chem,3f}$ atoms). In the rutile bulk structure of RuO_2 [29] the coordination is much higher compared to the chemisorption phase, albeit at a very similar bond length: Every Ru atom is surrounded by an octahedron of six oxygens with O–Ru bond lengths of 2.00 and 1.96 Å to the four basal and two apical oxygens respectively. On the other hand, the Ru coordination of O atoms in the chemisorbed state and in the bulk oxide structure is both threefold.

If the rutile RuO_2 is cut along the (1 1 0) plane, three distinct surface terminations are possible. The stoichiometric termination shown in Fig. 1b exhibits two types of atoms with truncated bonds, namely fivefold coordinated $Ru^{cus,5f}$ and twofold coordinated O^{bridge} atoms. As a result, both atoms relax inwards, which e.g. translates into a shortened bondlength of 1.91 Å between O^{bridge} and the underlying sixfold coordinated $Ru^{bridge,6f}$ atoms.

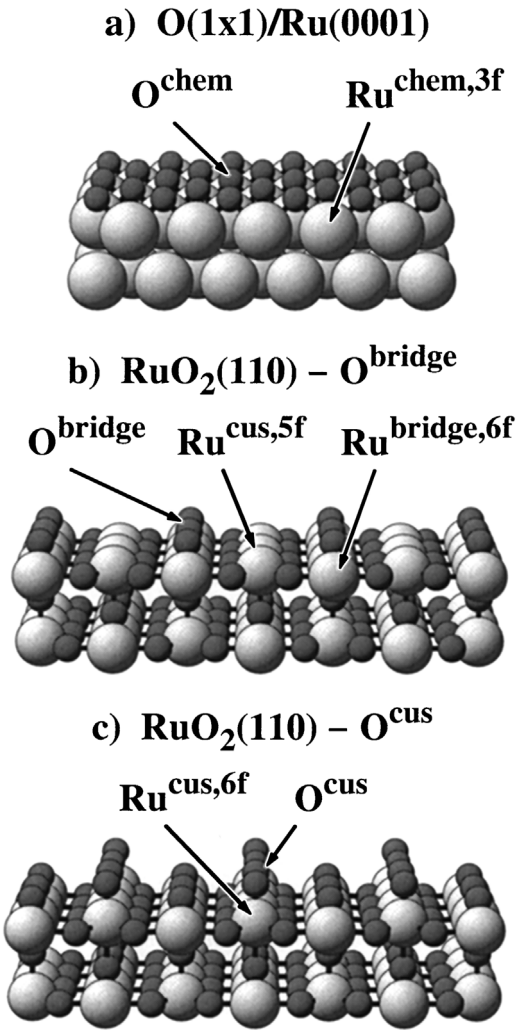

Fig. 1. Surface structures of domains on O-rich Ru(0 0 0 1). (a) Chemisorbed $O(1 \times 1)$/Ru(0 0 0 1) with threefold O^{chem} coordinated $Ru^{chem,3f}$ surface atoms. (b) Stoichiometric RuO_2(1 1 0)–O^{bridge} termination with five-, six- and twofold coordinated $Ru^{cus,5f}$, $Ru^{bridge,6f}$ and O^{bridge} atoms respectively. (c) High-pressure RuO_2(1 1 0)–O^{cus} termination, where additional O^{cus} atoms sit atop the formerly undercoordinated $Ru^{cus,6f}$ atoms (Ru – large, light spheres, O – small, dark spheres).

This termination (henceforth referred to as O^{bridge} termination) is traditionally believed to be the most stable one for (1 1 0) surfaces of all rutile-structured metal oxides [30], and in ultrahigh vacuum (UHV) it was also found on the oxide patches that had formed on the Ru(0 0 0 1) surface [3]. However, in recent calculations determining

the lowest energy structure in equilibrium with a given environment we found that this termination is only stable at a low O chemical potential [31]. Under more O-rich conditions a different termination (henceforth referred to as O^{cus} termination) is stabilized, in which terminal oxygen atoms, O^{cus}, occupy sites atop of the formerly coordinatively unsaturated $Ru^{cus,5f}$ atoms as shown in Fig. 1c. Although this achieves the bulk-like sixfold O coordination for the now $Ru^{cus,6f}$ atoms, the O^{cus}–$Ru^{cus,6f}$ bond length is due to the singly-bonded atop site with 1.70 Å significantly shorter than all aforementioned bond lengths in the O/Ru system.

By post-dosing the $RuO_2(1\,1\,0)$ surface with additional O at room temperature this high-pressure termination of $RuO_2(1\,1\,0)$ has recently also been created and characterized in UHV intentionally [32,33]. However, depending on the details of the experimental preparation we are convinced that this high-pressure termination was probably also present in a number of previous studies addressing $RuO_2(1\,1\,0)$, in particular the ones where the oxide was treated under O-rich conditions without a final annealing step [1,2,15,28]. We finally note in passing, that our calculations show that the third possibility of terminating a RuO_2-$(1\,1\,0)$ crystal with a mixed (RuO) layer exhibited at the surface is never realized in the range of possible O chemical potentials.

4. Results

4.1. Surface core-level shifts for $RuO_2(1\,1\,0)$

Aiming at a fingerprint guidance for XPS experiments, we concentrate on the discussion of the photoemission from those atoms, for which rather large SCLSs are expected due to a significantly changed local environment with respect to the bulk situation (cf. Table 1 and Fig. 1). From an inspection of the initial-state SCLSs we estimate that the peaks due to all other atoms, which are located in deeper surface layers, will lie closer than $\approx\pm 0.2$ eV around the respective RuO_2 bulk peak. Note, that in our sign convention a positive SCLS indicates a shift towards higher binding energies, i.e. the core level moves away from the Fermi level. Similarly, a positive screening contribution to the total shift occurs, if the created core hole is less screened at the surface than in the bulk.

Table 1
Calculated Ru 3d and O 1s SCLSs on $RuO_2(1\,1\,0)$

Termination		Total	Screening	Initial
Ru 3d SCLSs in eV				
O^{bridge}	$Ru^{bridge,6f}$	+0.29	−0.15	+0.44
	$Ru^{cus,5f}$	−0.16	−0.02	−0.14
O^{cus}	$Ru^{bridge,6f}$	+0.40	−0.14	+0.54
	$Ru^{cus,6f}$	+1.37	+0.07	+1.30
O 1s SCLSs in eV				
O^{bridge}	O^{bridge}	−0.87	−0.68	−0.19
O^{cus}	O^{bridge}	−0.97	−0.77	−0.20
	O^{cus}	−0.79	−0.98	+0.19

Shown are the total shifts, as well as their decomposition into screening and initial state parts: $\Delta^{total}_{SCLS} = \Delta^{screen} + \Delta^{initial}_{SCLS}$.

Concentrating first on the Ru 3d SCLSs in the stoichiometric $RuO_2(1\,1\,0)$–O^{bridge} termination we find only rather modest shifts for both the $Ru^{bridge,6f}$ and the $Ru^{cus,5f}$ atoms. While this is not very surprising for the former atom, which possesses its sixfold bulk-like O coordination (albeit with a reduced bond length to the O^{bridge} atoms), one could have imagined a larger shift for the $Ru^{cus,5f}$ atoms, which after all lack their atop apical oxygen neighbour. However, these atoms are considerably relaxed inwards, reinforcing the backbond to the underlying second apical O at a reduced bond length of 1.88 Å. Thus, the bond truncation and backbond strengthening seem to balance up, leading in total to an almost bulk-like situation and in turn to a very small SCLS.

The final-state contribution for both atoms is negative, indicative of a more efficient screening at the surface. A similar screening behaviour was already found for all Ru surface atoms in the O adlayer phases on metallic Ru(0 0 0 1) and explained by an enhanced d density of states (DOS) around the Fermi level [25]. Upon core excitation, the 4d-band shifts to lower energies, causing a valence electron from the Fermi reservoir to restore local charge neutrality by filling up formerly unoccupied d-states. In turn, if the d-DOS at and above the Fermi level is higher for a surface atom than for a bulk atom, a more efficient screening results. Inspecting the d-DOS of both $Ru^{bridge,6f}$ and $Ru^{cus,5f}$,

we indeed find again such an enhancement, confirming that not only in the Ru metal, but also in its oxide the final-state effect is mainly due to intra-atomic d-electron screening.

In the $RuO_2(1\,1\,0)$–O^{cus} termination, the $Ru^{bridge,6f}$ SCLS remains almost unchanged, which is intelligible as the addition of the terminal O^{cus} atoms does not directly influence the nearest-neighbour coordination of this Ru surface atom (cf. Fig. 1c). However, the $Ru^{cus,6f}$ atoms are of course significantly affected, exhibiting now a large shift of +1.37 eV towards higher binding energies. As apparent from Table 1 this shift is primarily an initial-state effect, which we attribute to the very short bond length of 1.70 Å formed to the atop O^{cus} atoms. Yet, also the $Ru^{cus,6f}$ d-DOS at the Fermi level is lowered so strongly by the new bond, that we additionally observe a sign reversal in the screening contribution. Reflecting a reduced screening capability at the surface the final-state effect points thus in the same direction as the large initial-state shift, further augmenting the total SCLS. Note, that we had previously observed such a change in the screening behaviour also at high coverage O adlayers on Rh(1 1 1), where the oxygen–metal interaction likewise reduced the d-DOS at the Fermi level below the corresponding bulk value [34]. The resulting very large SCLS for the $Ru^{cus,6f}$ atoms in this hitherto unaccounted high-pressure termination is related to a long standing controversy concerning the interpretation of XPS data on $RuO_2(1\,1\,0)$, which detailed discussion we defer to the following section.

Turning our attention to the O 1s shifts, we immediately recognize that contrary to the situation for the Ru 3d's, the total SCLSs are now predominantly determined by a large, negative screening contribution. The initial-state shifts on the other hand are almost bulk-like, with O^{bridge} atoms showing very similar values in both terminations. The strongly enhanced screening at the surface is due to dangling-bond type states on both surface oxygens as reflected in the DOS shown in Fig. 2. These oxygen–metal states, which are concentrated on O^{bridge} and O^{cus} and their respective directly bonded $Ru^{bridge,6f}$ and $Ru^{cus,6f}$ neighbours, fall in the energy region $-8.0 < E < -2.0$ eV in bulk RuO_2 [29], but are shifted towards the Fermi level due to the bond truncation at the surface. There they strongly enhance the DOS and thus induce the large negative screening contribution to the O 1s SCLSs.

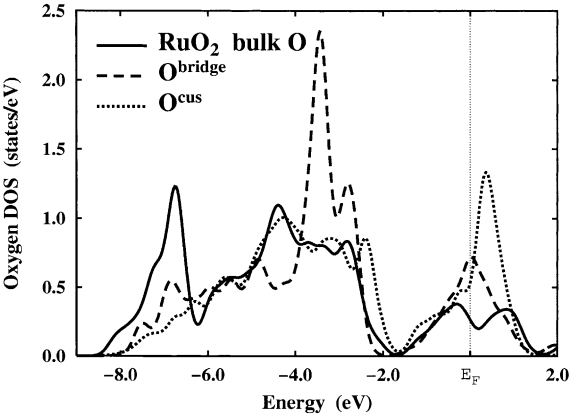

Fig. 2. Calculated DOS for bulk O in RuO_2 (solid line), as well as for O^{bridge} and O^{cus} atoms (dashed and dotted lines respectively) in the $RuO_2(1\,1\,0)$–O^{cus} termination. The O^{bridge} DOS in the $RuO_2(1\,1\,0)$–O^{bridge} termination is almost identical to the one shown here. The energy zero is at the Fermi level.

4.2. The satellite peak discussion

Motivated by the widespread use of RuO_2 as catalyst for electrochemical, as well as organic and inorganic processes, a large number of studies has already applied low-resolution XPS to elucidate the oxide's surface structure and composition (Refs. [8–15] and references therein). Even at the resolution of a Mg/Al X-ray source the Ru 3d spectrum of $RuO_2(1\,1\,0)$ clearly shows an additional rather broad peak at about $+1.7 \pm 0.1$ eV to the higher binding energy side of each of the primary 3/2 and 5/2 components [12,14,15]. Under the assumption that the large shift of this peak indicates a significant deviation of the local environment of the emitting atom with respect to the bulk phase, the satellite was at first assigned to the presence of a higher oxidation state of Ru at the surface, namely Ru^{6+} in a RuO_3 type oxide structure [8–12]. Concomitantly, this interpretation resulted even in the inclusion of a Ru $3d_{5/2}$ binding energy for RuO_3 in a common XPS handbook [35]. However, more recent work has questioned the

existence of this conjectured surface oxide, which is not known to be stable as a bulk phase [14,15]. In particular, a recent analysis of XPD azimuthal scans by Kim et al. showed that the photoelectrons in the satellite peaks originate from a rutile-type environment [15], which is an unlikely structure for the presumed RuO_3.

Alternatively, Cox et al. [14] attributed the satellite peak to final-state screening effects. As outlined in the previous section, the core hole created in the photoemission process pulls down formerly unoccupied valence band DOS below the Fermi level. The photoemission spectrum may then exhibit a multiple peak structure, often called the Kotani–Toyozawa effect [36,37]. The high kinetic energy peak reflects the possibility that electron transfer into the shifted DOS happens fast enough to impart the corresponding screening energy onto the emitted photoelectron (this corresponds to the fully-screened results of our calculations). And the low-energy peak reflects the possibility that the shifted DOS remains unoccupied on the time scale of the emission process. Of course, in addition there is also the possibility of even lower kinetic energy structures than this "unscreened peak" because the emitted photoelectron may also loose energy, e.g. by creating surface plasmons. The Kotani–Toyozawa effect has been observed in photoemission from systems with highly localized f or 3d valence band states [38]. However, the good overlap and spatial extension of the 4d wave functions in RuO_2 (the width of the shifted DOS peak is about 1 eV) suggests that the screening dynamics will be fast. Thus, the probability (i.e., the intensity) of this unscreened final-state peak should be low. Furthermore, our calculations show that the screening energy is small for emission from Ru core levels (cf. Table 1). Thus, even if a Kotani–Toyozawa peak existed at the higher binding energy side, it would be shifted by less than 0.2 eV with respect to the peak due to the fully screened final state, which is not enough to account for the well separated satellite seen in the experiments.

On the other hand, for photoemission from the oxygen atoms, the dynamics of screening could be interesting. The nodeless O 2p states are very localized and the calculated screening energy is large. Consequently, the screened and unscreened surface peaks of the photoemission spectrum would be well separated. While the latter overlap (at least partly) with the bulk peak, the fully screened final-state peaks are noticeably shifted to higher kinetic energy. Hence, high-resolution O 1s photoemission focussing on the low binding energy side of the bulk peak (i.e. the peak shape) could provide important information on the many-body dynamics of the photoemission process of this system.

Coming back to the Ru 3d satellite peak issue, we suggest in light of the SCLS analysis presented in the previous section, that it is neither due to RuO_3, nor due to the unscreened emission, but receives a signal from the $Ru^{cus,6f}$ atoms in the $RuO_2(1\,1\,0)$–O^{cus} high-pressure termination. Although the calculated large shift of $+1.37$ eV agrees at first sight only semiquantitatively with the experimentally reported 1.7 ± 0.1 eV (cf. the compilation of measured XPS data in Ref. [13]), one has to keep in mind that all these studies were done with low-resolution XPS on rather ill-defined samples, the majority even on polycrystalline material. In particular, none of the studies was performed on single-crystal $RuO_2(1\,1\,0)$, but always involving either oxidized Ru or grown RuO_2 thin films, both bearing a certain likelihood for the presence of unoxidized Ru remnants on the surface. As we will show below, the metallic Ru bulk peak lies to the lower binding energy side of the RuO_2 bulk peak, with all surface peaks due to Ru coordinated to chemisorbed oxygen in between. Unresolved, these peaks will lead to an erroneous RuO_2 bulk peak determination at too low a binding energy and in turn to an overestimation of the total shift to the satellite peak, possibly explaining the 0.3 eV difference to our result.

Asides, the assignment of the satellite peak as a fingerprint for the hitherto simply not conceived high-pressure $RuO_2(1\,1\,0)$–O^{cus} termination would be fully compatible with the reported experimental sample preparations, which unanimously involve highly oxidizing conditions. After the transfer to UHV the O^{cus} atoms are stable up to about 450 K [39], so that the high-pressure termination is most likely frozen in, if not a final annealing step is performed as e.g. in the LEED work by Over and coworkers [3–5]. The $Ru^{cus,6f}$ atoms in the

$RuO_2(1\,1\,0)$–O^{cus} termination are also obviously situated in a rutile-type environment, thus explaining the aforementioned XPD results of Kim et al. [15]. Finally, we notice that our present model does not exclude the possibility that a many-body peak, e.g. due to a surface plasmon loss, falls in the same energy region, then being the predominant source of the satellite peak. At present, we can only state that the screened emission from $Ru^{cus,6f}$ atoms - resolved or unresolved - contributes to the signal at the corresponding energy. Whether this is the sole explanation for the satellite peak or not, can only be determined by a high-resolution XPS study on single-crystalline $RuO_2(1\,1\,0)$, which we hope to encourage with the present work.

4.3. XPS fingerprinting of the oxidation sequence

Having completed the analysis of the oxidic SCLSs, we proceed to compare them with the peaks that arise from metallic Ru surface atoms coordinated to chemisorbed O. Since our intention focusses on describing the XPS trends during the oxidation of a Ru(0 0 0 1) surface, we now reference all Ru 3d and O 1s SCLSs with respect to the initially present peaks due to bulk metallic Ru and chemisorbed $O^{chem,3f}$ in the $O(1\times1)$/Ru(0 0 0 1) phase respectively. Again we stress that the shift between metallic and oxidic bulk peaks cannot be determined as accurately as the individual SCLSs on the respective surfaces and that we aim now more at the trends than at ironclad numbers. On the other hand, note that on a qualitative level our results even describe already the existing data from polycrystalline samples [8,9,13], Ru(0 0 0 1) being the most stable surface orientation.

In our previous work addressing the ordered O overlayers on Ru(0 0 0 1) we had shown that the progressive O chemisorption leads to a Ru 3d shift towards higher binding energies, which scales linearly with the number of direct O neighbours coordinated to the respective Ru surface atoms [25]. For the final $O(1\times1)$/Ru(0 0 0 1), which in turn is precedent to and coexisting with already fully oxidized patches on an O-rich Ru(0 0 0 1) surface [4], this results in a SCLS of +0.90 eV for the $Ru^{chem,3f}$ atoms as shown in Fig. 3a (cf. with the atomic structure displayed in Fig. 1a). On the contrary, we find the O 1s level almost constant to within +0.18 eV in all four adlayer structures, indicating that the always threefold coordinated $O^{chem,3f}$ remains essentially in the same chemical state apart from a slightly increased repulsion due to the more and more close packing of the electronegative adsorbates in the higher coverage phases.

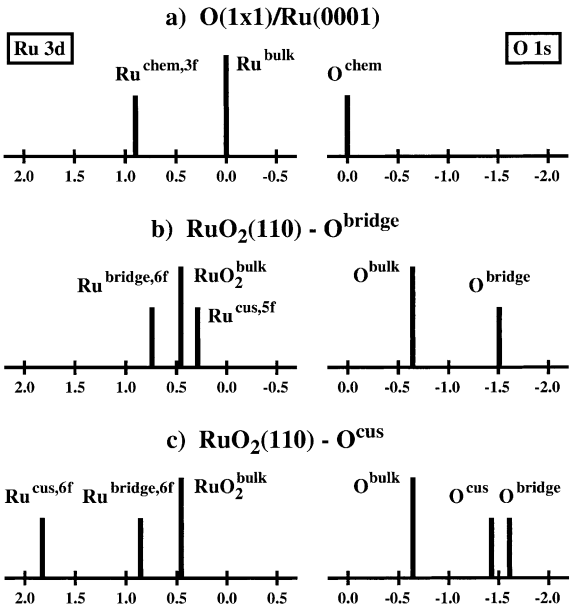

Fig. 3. Computed fully-screened Ru 3d and O 1s SCLSs for the three domain types on an oxygen-rich Ru(0 0 0 1) surface. Ru in the metallic bulk and O in the $O(1\times1)$/Ru(0 0 0 1) phase are used as zero reference. Units are eV.

With the given accuracy caveat, we determine the Ru 3d peak due to bulk RuO_2 at +0.46 eV on the higher binding energy side of the metallic Ru peak, which compares well with the polycrystalline XPS literature value of $+0.7\pm0.1$ eV [13]. As apparent in Fig. 3b all Ru 3d peaks due to the UHV $RuO_2(1\,1\,0)$–O^{bridge} termination will thus fall between the $Ru^{chem,3f}$ peak due to the Ru surface atoms in the just described $O(1\times1)$/Ru(0 0 0 1) phase and the metallic Ru bulk peak. In contrast, emission from the $Ru^{cus,5f}$ atoms in the RuO_2-(1 1 0)–O^{cus} termination will lead to the well separated satellite peak discussed in the previous section, cf. Fig. 3c, therewith offering a fingerprint for the existence of this domain type on the

surface. With the presence of oxides on the surface the Ru 3d XPS spectrum will therefore clearly be shifted towards higher binding energies as more spectral weight is transferred to the oxidic peaks. Yet, even with a high-resolution X-ray source it will be very difficult to distinguish between coexisting $RuO_2(1\,1\,0)$–O^{bridge} and $O(1\times1)$/Ru(0 0 0 1) domains.

This distinction will be much more clearcut in the O 1s XPS spectrum. The peak due to RuO_2 lattice oxygen appears at -0.64 eV towards lower binding energies, so that the largely shifted surface peaks of both oxide terminations show a total displacement of ~-1.5 eV. While this will thus not allow to determine which surface termination is present on the oxidic domains, the existence of the latter on the surface (even to a very small degree) will be easily monitored by the appearance of these new, well-separated peaks in the O 1s spectrum. Together with the Ru 3d satellite peak as a fingerprint for the high-pressure termination, all three domains should thus be clearly distinguishable by XPS, confirming our initial statement that the latter technique is a well suited tool to study the initial stages of the oxidation of the Ru(0 0 0 1) surface.

5. Summary

The oxidation of the Ru(0 0 0 1) surface proceeds via the $O(1\times1)$ chemisorption phase before $RuO_2(1\,1\,0)$ domains start to form. From a calculation of the corresponding SCLSs we predict a shift of the Ru 3d (O 1s) XPS spectrum towards higher (lower) binding energies as soon as oxide domains are present. In particular O 1s XPS will be a very sensitive tool to study the onset of the oxidation process, as the corresponding large shift results in the appearance of new peaks. The Ru 3d spectrum of $RuO_2(1\,1\,0)$ exhibits a clearly separated satellite peak at the higher binding energy side, which we assign to the existence of a hitherto unaccounted high-pressure termination. In this termination, terminal O^{cus} atoms sit atop of the formerly coordinatively unsaturated (cus) $Ru^{cus,5f}$ atoms of the stoichiometric $RuO_2(1\,1\,0)$ termination, normally believed to be the most stable truncation of all rutile (1 1 0) crystals. The very short bond length between the O^{cus} and $Ru^{cus,6f}$ atoms significantly deviates from the bulk-like situation, leading to a large initial-state shift of the core-level of the latter and thus possibly causing the long disputed satellite peak.

Acknowledgements

Stimulating discussions with Artur Böttcher and Horst Conrad are gratefully acknowledged.

References

[1] A. Böttcher, H. Niehus, S. Schwegmann, H. Over, G. Ertl, J. Phys. Chem. B 101 (1997) 11185.
[2] A. Böttcher, H. Conrad, H. Niehus, Surf. Sci. 452 (2000) 125.
[3] H. Over, Y.D. Kim, A.P. Seitsonen, S. Wendt, E. Lundgren, M. Schmid, P. Varga, A. Morgante, G. Ertl, Science 287 (2000) 1474.
[4] Y.D. Kim, A.P. Seitsonen, H. Over, Surf. Sci. 465 (2000) 1.
[5] Y.D. Kim, H. Over, G. Krabbes, G. Ertl, Topics in Catalysis 14 (2001) 95.
[6] C.H.F. Peden, D.W. Goodman, J. Phys. Chem. 90 (1986) 1360.
[7] K. Reuter, C. Stampfl, M.V. Ganduglia-Pirovano, M. Scheffler, Phys. Rev. Lett., submitted for publication.
[8] K.S. Kim, W.E. Baitinger, J.W. Amy, N. Winograd, J. Electron Spectrosc. Rel. Phenom. 5 (1974) 351.
[9] H.J. Lewerenz, S. Stucki, R. Kotz, Surf. Sci. 126 (1983) 893.
[10] R. Kotz, H.J. Lewerenz, S. Stucki, J. Electrochem. Soc. 130 (1983) 825.
[11] W.E. O'Grady, Lj. Atanasoska, F.H. Pollak, H.L. Park, J. Electronal. Chem. 178 (1984) 61.
[12] Lj. Atanasoska, W.E. O'Grady, R.T. Atanasoski, F.H. Pollak, Surf. Sci. 202 (1988) 142.
[13] H.Y.H. Chan, C.G. Takoudis, M.J. Weaver, J. Catal. 172 (1997) 336.
[14] P.A. Cox, J.B. Goodenough, P.J. Tavener, D. Telles, R.G. Egdell, J. Solid State Chem. 62 (1986) 360.
[15] Y.J. Kim, Y. Gao, S.A. Chambers, Appl. Surf. Sci. 120 (1997) 250.
[16] J.P. Perdew, S. Burke, M. Ernzerhof, Phys. Rev. Lett. 77 (1996) 3865.
[17] P. Blaha, K. Schwarz, J. Luitz, WIEN97, A Full Potential Linearized Augmented Plane Wave Package for Calculating Crystal Properties, Karlheinz Schwarz, Techn. Universität Wien, Austria, 1999, ISBN 3-9501031-0-4.
[18] B. Kohler, S. Wilke, M. Scheffler, R. Kouba, C. Ambrosch-Draxl, Comput. Phys. Commun. 94 (1996) 31.

[19] M. Petersen, F. Wagner, L. Hufnagel, M. Scheffler, P. Blaha, K. Schwarz, Comp. Phys. Commun. 126 (2000) 294.
[20] C. Stampfl, S. Schwegmann, H. Over, M. Scheffler, G. Ertl, Phys. Rev. Lett. 77 (1996) 3371.
[21] D. Spanjaard, C. Guillot, M.C. Desjonqueres, G. Treglia, J. Lecante, Surf. Sci. Rep. 5 (1985) 1.
[22] W.F. Egelhoff, Surf. Sci. Rep. 6 (1987) 253.
[23] J.F. Janak, Phys. Rev. B 18 (1978) 7165.
[24] J.P. Perdew, M. Levy, Phys. Rev. B 56 (1997) 16021.
[25] S. Lizzit, A. Baraldi, A. Groso, K. Reuter, M.V. Ganduglia-Pirovano, C. Stampfl, M. Scheffler, M. Stichler, C. Keller, W. Wurth, D. Menzel, Phys. Rev. B 63 (2001) 205419.
[26] C. Stampfl, M. Scheffler, Phys. Rev. B 54 (1996) 2868.
[27] D. Menzel, Surf. Rev. Lett. 6 (1999) 835.
[28] A. Böttcher, H. Niehus, J. Chem. Phys. 110 (1999) 3186.
[29] P.I. Sorantin, K.H. Schwarz, Inorg. Chem. 31 (1992) 567.
[30] V.E. Henrich, P.A. Cox, The Surface Science of Metal Oxides, Cambridge University Press, Cambridge, 1994.
[31] K. Reuter, M. Scheffler, Phys. Rev. B, submitted for publication.
[32] Y.D. Kim, A.P. Seitsonen, S. Wendt, J. Wang, C. Fan, K. Jacobi, H. Over, G. Ertl, J. Phys. Chem. B 105 (2001) 3752.
[33] C.Y. Fan, J. Wang, K. Jacobi, G. Ertl, J. Chem. Phys. 114 (2001) 10058.
[34] M.V. Ganduglia-Pirovano, M. Scheffler, A. Baraldi, S. Lizzit, G. Comelli, G. Paolucci, R. Rosei, Phys. Rev. B 63 (2001) 205415.
[35] J.F. Moulder, W.F. Stickle, P.W. Sobol, K.D. Bonben, Handbook of X-ray Photoelectron Spectroscopy, Perkin–Elmer, Physical Electronics Division, 1992.
[36] A. Kotani, Y. Toyozawa, J. Phys. Soc. Jpn. 35 (1973) 1073.
[37] A. Kotani, Y. Toyozawa, J. Phys. Soc. Jpn. 37 (1974) 912.
[38] A. Kotani, J. Electron Spectrosc. Rel. Phenom. 100 (1999) 75.
[39] A. Böttcher, H. Niehus, Phys. Rev. B 60 (1999) 14396.